JOURNAL OF MECHANICAL ENGINEERING, SCIENCE, AND INNOVATION
ITATS
Research Article

Wavy Leading Edge (WLE) Influence on a Rectangular Wing Using an Unsteady Analysis Approach

Journal of Mechanical Engineering, Science, and Innovation
e-ISNN: 2776-3536
2023, Vol. 3, No. 1
DOI: 10.31284/j.jmesi.2023.v3i1.4477
ejurnal.itats.ac.id/jmesi

Iis Rohmawati[1,2], Hiroshi Arai[3], and Ika Nurjannah[4]

[1]Hiroshima University, Japan.
[2]Meiji University, Japan.
[3]Japan Marine Corporation, Japan.
[4]Universitas Negeri Surabaya, Indonesia.

Corresponding author:
Iis Rohmawati
Meiji University
Email: rohmawati@meiji.ac.jp

Abstract

A rectangular wing with Wavy Leading Edge (WLE) effect was investigated experimentally and numerically. This research was carried out with the NACA 0018 profile. The morphology of humpback whale flippers, which are blunt and rounded in a specific pattern, inspired the design of the WLE. The rectangular wing was explored in pitching motion with a reduced frequency of k = 0.25 and varied aspect ratios. Multiple aspect ratios (AR) of the rectangular wing have been evaluated to determine the best wing aspect ratio, notably 3.9, 5.1, and 7.9. Only at AR 3.9 and 5.1 does the WLE perform efficiently in both upstroke and downstroke motion. WLE has a sinusoidal function shape. The improvement of lift force was stronger during upstroke motion than during downstroke motion. The stall is minimized during the pitching motion of the WLE wing, according to the numerical simulation. This result could be applied to fin stabilizers or wind turbines.

Keywords: *Wavy Leading Edge, pitching motion, rectangular wing, NACA 0018.*

Received: May 3, 2023; Received in revised: May 31, 2023; Accepted: May 31, 2023
Handling Editor: Hasan Maulana

INTRODUCTION

Inspired by the humpback whales, which have the shape streamlined, blunt, and rounded flipper morphology contributing to their ability to catch prey, there has been interest in applying this shape to improve hydrodynamic performance in various applications like fin stabilizers, aircraft, and wind turbines. It is necessary to ensure good performance through improvements in hydrodynamics. One approach to improving

Figure 1. Uniqueness of flipper on humpback whale [1]

hydrodynamics is through the use of flow control devices, which can be classified based on their energy expenditure as either active or passive controls. In this research, we are focused on passive control by adding Wavy Leading Edge (WLE) on the hydrofoil. One passive control method involves using a WLE attached to the wing to improve hydrodynamic performance. By imitating the flipper shape of the humpback whale, scientists have developed various wing shapes, including rectangular and taper wings. This study examines and compares the utilization of the wavy leading edge in rectangular wing form.

Previous research on applying passive control methods for fluid flow, like adding WLE on a wing and utilizing as a turbulent generator, is discussed in the paragraph below. Formerly, research had been conducted based on the design of the humpback whale's flipper. According to Fish et al. [2], the humpback whale flipper shape is designed for excellent mobility, essential for the whale's distinctive feeding activity. As seen in Figure 1, its flipper uses tubercles as passive control devices, while its cross-sectional design resembles the aerodynamic foils that generate lift

Fish et al [3] pioneered the use of bio-inspired technology, demonstrating that the existence of tubercles on finite wing models can delay the stall. This will be resulting in enhanced maximum lift and less drag. They highlighted natural passive techniques to alter fluid flow to delay stall and boost lift while reducing drag [4] the tubercles for passive flow control have the potential design for wings, fans, and wind turbines. Miklosovic et al. [5-6] conducted another investigation to a scalloped flipper. They obtained their method can postpone stall location and improve lift force. The scalloped flipper exceeded the full span type in delaying stall. However, the mechanism causing the stall remains undetermined.

The main objective of this study was to apply WLE as fin stabilizers and wind turbines. These tools suffer from dynamic stall caused by unsteady motion. Therefore, the aspect ratio is playing important rule at it. The unsteady analysis will be performed for aspect ratios of 3.9, 5.1, and 7.9. The rectangular wings attached at NACA 0018 profiles and chord lengths c of 125 mm were employed. The WLE has an 8% c wavelength and a 5% c amplitude.

Pedro et al. [7] compared experimentally and computational studies to examining the performance of scalloped and smooth flippers at Reynolds number 5 x 105. By understanding how separation affects wing performance, the Spalart-Allmaras RANS turbulence model was investigated at aerodynamic performance. The scalloped flipper was more effective than the smooth flipper for resisting separation.

Johari et al. [8] investigated the effect of leading-edge sinusoidal protuberances on the lift, drag, and pitching moments of airfoils in a water tunnel, compared to a baseline 634-021 airfoil. Their study made use of sinusoidal protuberances applied to the front edge of the wing. Airfoils with leading-edge protuberances did not experience the stall in the same manner as the baseline foil with a smooth leading edge. The amplitude of the

protuberances had an important impact on airfoil performance, while the wavelength indicates the waviness of the leading edge that did not significantly impact improving the wing performance. It is essential to emphasize that their research was carried out under steady conditions and the mechanism of the flow pattern was not noticed.

Arai et al. [9-10] utilized a circular water channel and a NACA0018 profile to investigate the delaying stall mechanism. They utilized numerical simulations with an LES turbulence model to generate displayed lift and drag coefficients that agreed well with the experimental results. According to the findings on rectangular wings, a shorter protuberance wavelength generates greater lift force at post-stall angles of attack. When compared to a baseline wing with a pre-stall angle of attack, a wing featuring a wavy leading edge exhibits a lower maximum lift value. The WLE wing is more resistant to separation under post-stall conditions.

Wei et al. [11] recently investigated the flow structures of wings at moderate aspect ratios (AR = 4) at leading-edge tubercles. They employed a NACA634-021 profile with leading-edge tubercles. Thus, they obtained numerically the wing configurations with tubercle characteristics i.e. amplitude and wavelength. Larger tubercle amplitudes resulted a progressive stall. Although thus smaller tubercle wavelengths enhanced maximum lift. In addition, recirculating bubbles increase and apparent inboard spanwise flows, which those were linked to flow due to the tip vortex.

Wang et al. [12] used studied the NACA 0010 numerically to obtained the static effect of leading-edge protuberances and pitching wing. The protuberances function as vortex generators. Thus, it causing the increasing momentum at the boundary layer and delaying stall. However, they simulated those conditions, the leading-edge protuberances have little impact on a pitching wing.

The studies above have primarily focused on the influence of WLEs on wings in steady-state conditions specific wing forms. The investigation effects of WLEs were at the tapering wings and it appear in unstable cases, notably pitching motion. Its rotating motion is applicable for wind turbine and helicopter propeller. The unsteady motion revelas the potential benefits of WLEs such as fin stabilizers and other wing shapes. More research reveal the full potential of WLE application on various wing shapes.

The investigation to the wavy leading edges by unsteady condition is limited. However, the potential benefits of such research could be applied to a variety of applications, like fin stabilizers and wind turbines. To optimize its applications, the influence of WLE in unsteady conditions is attractive studied. The wing's aspect ratio is also significant in determining how WLE affects lift and drag. The purpose of this study is to investigate the wing performance by adding the WLE at various aspect ratios. The idea is to increase lift while decreasing drag. The study appears into the mechanism of stall delay produced by WLE as well.

METHODS

Wing Scheme

The main configuration of this study was NACA 0018 profile. In this study, the NACA 0018 profile with a chord length of 125 mm and aspect ratios (AR) of 3.9, 5.1, and 7.9 was chosen. Figure 2 shows the coordinate system of the wing. Thus, the set point (*O-xyz*) positioned at the leading edge. The aspect ratio (AR) regards to their dimensions. The wing was adding a wavy leading edge, as shown in Figure 3.

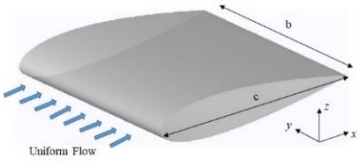

Figure 2. Coordinate system

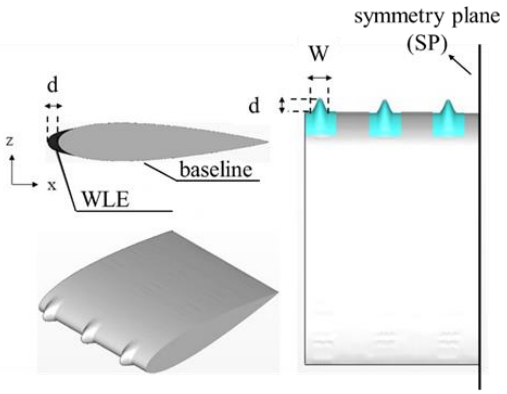

Figure 3. WLE's schematic view

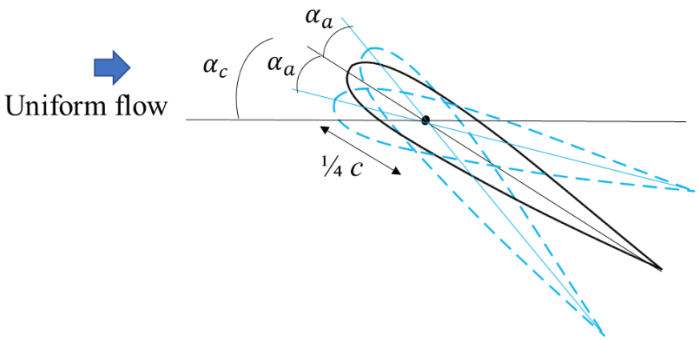

Figure 4. Pitching motion

The formula used to establish the configuration of the WLE is as follows:

$$x_{WLE\,(y)} = x_{LE} - [\frac{d}{2}\sin\left\{\frac{2\pi}{W}\left(y - \frac{W}{4}\right)\right\} + \frac{d}{2}] \quad (1)$$

The following variables was set at the wavy leading edge: The baseline wing's x-coordinate is x_{LE}, the wavy leading edge's x-coordinate is represented by x_{WLE}, and the width and height of the wavy leading edge are represented by W and d, respectively. In this investigation, d and W were set to 5% of the chord length and 8%, respectively. The wing motion was characterized by the following equation in both steady and unsteady cases:

$$\alpha\,(T_0) = \alpha_c + \alpha_a \cos\,(k\,T_0) \quad (2)$$

Where α, α_c , α_a indicates the angle of attack, center angle, and amplitude, respectively.

The parameter T_0 indicates non-dimensional time with a reduced frequency k = 0.25 employed in this study based on the RORO ship's fin stabilizer motion. The following are the equations for T_0 and k:

$$T_0 = t\frac{U_0}{c} \quad (3)$$

$$k = \frac{2\pi f c}{U_0} \quad (4)$$

Where t, c, f, and U_0 are time, wing chord length, frequency, and free stream velocity, respectively.

Table 1. Experiment Configuration

Wing profile	**NACA 0018**
Aspect Ratio	3.9, and 5.1
Reynolds Number (*Re)*	1.4 x 10^5
Reduced Frequency (*k)*	0.25
Mean angle of pitch motion (α_c)	20° and 30°
Amplitude of pitch motion (α_a)	5°

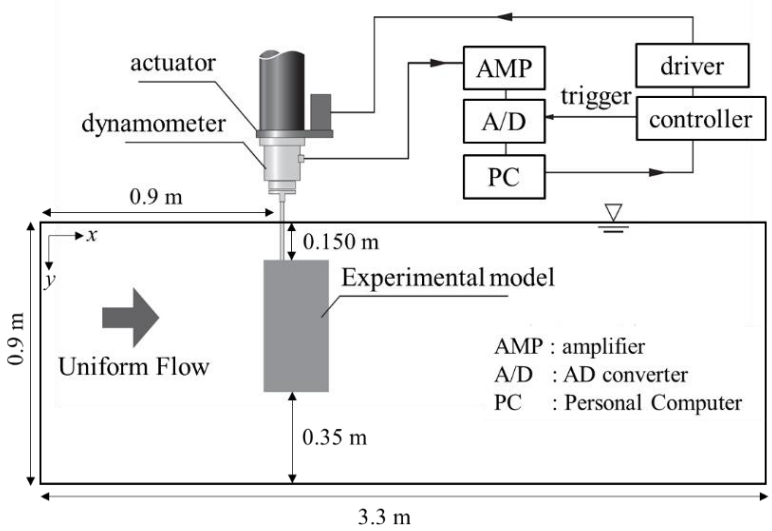

Figure 5. Experimental set-up

Figure 4 shows the wing motion by moving up and down. Thus, the pivot point positioned at a quarter of the chord length.

Experimental Method

The experiments are employed at a circular water channel with a width of 1.4 m, a height of 1.0 m, and a measuring cross-section of 3.3 m, as shown in Figure 5. At a depth of 0.9 m in the circular water channel, the wing is 0.9 m from the uniform flow and 0.15 m from the upper surface. The experiments were limited between AR 3.9 and 5.1 due to the size restrictions of the circular water channel. The chord length of the wing was set to c = 0.125 m for AR 3.9 and 5.1 to maintain an identical ratio between the wing and the bottom of the circular water channel. This ratio is known as the blockage ratio, and it was 8% between the wing and the outer boundary. The following is the definition of the blockage ratio:

$$\text{Blockage ratio} = \frac{AR\ c^2}{d} \tag{5}$$

Where AR, c, and d is the aspect ratio, chord length, and depth of outer boundary, respectively.

The experimental details are summarized in Table 1. The NACA 0018 profile with a Reynolds number of about 1.4 x 10^5 was used. The experimental method was performed by using circular water channel as described in Figure 5. The uniform flow is coming from the left side then flowing through the wing that placed at 0.9 m from the inlet. The wing

pitches angles was ranging from 25° to 35°. It flapped up and down according to the amplitude angle.

Numerical Method

In this research, Autodesk® CFD applies the numerical method. The procedure for conducting Autodesk® CFD computation involves the following steps: model construction, definition of model type, initialization of boundary conditions, meshing of the model into smaller parts, computation solution for either steady or unsteady cases, and analysis and visualization of the results.

For all investigation, the Unsteady Reynolds Averaged Navier-Stokes (URANS) equations with the SST k-ω turbulence model were used. This turbulence model, according to Wang et al. [13], can capture the flow of a dynamic stall. In their research, the SST k-ω were examined and shown to be useful for research purposes for low Reynolds number airfoils and VAWTs (Vertical Axis Wind Turbines). Based on experimental evidence, they can capture a considerable portion of the flow dynamics. Other references [14-18] have also conducted numerical studies in unsteady motion using the SST k-ω turbulence model. These experiments demonstrated that the modeling forces and flow structures accorded well with the experimental data.

In this study, the unstructured meshing approach with a trapezoidal mesh form was used. Ten layers were used to provide more precise flow patterns near the wing surface. Figures 6-7 show the mesh configuration of the baseline wing. The layer thicknesses shown in those figures ensured that y^+ was always less than 3. The mesh was improved with a growth ratio of about 1.05 to improve mesh generation towards the wing's outer margin. The total number of meshes employed was approximately 10 million, and the WLE wing simulation used an identical mesh design in all cases, with 10 layers and y^+ less than 3.

Figure 8 illustrates the steady and unsteady simulations of the domain with a 3.9 aspect ratio. The input boundary condition is uniform velocity, the downstream outlet is pressure, and the remaining boundaries are set to symmetry. A rotating region with a motion corresponding to a reduced frequency of k = 0.25 is present in the unsteady condition.

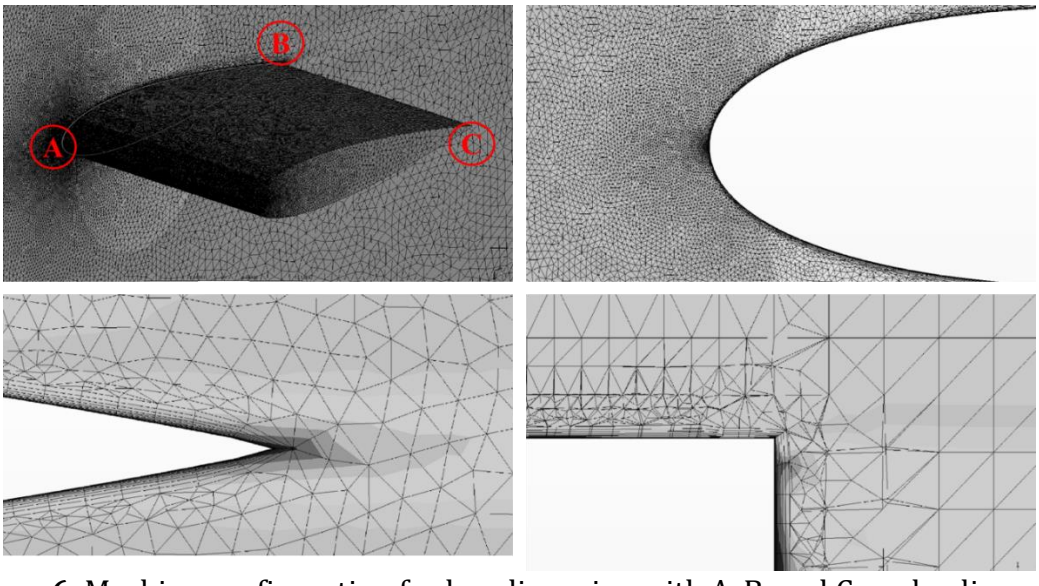

Figure 6. Meshing configuration for baseline wing with A, B, and C are leading edge, trailing edge that located at the symmetry plane, trailing edge at the top direction of the wing.

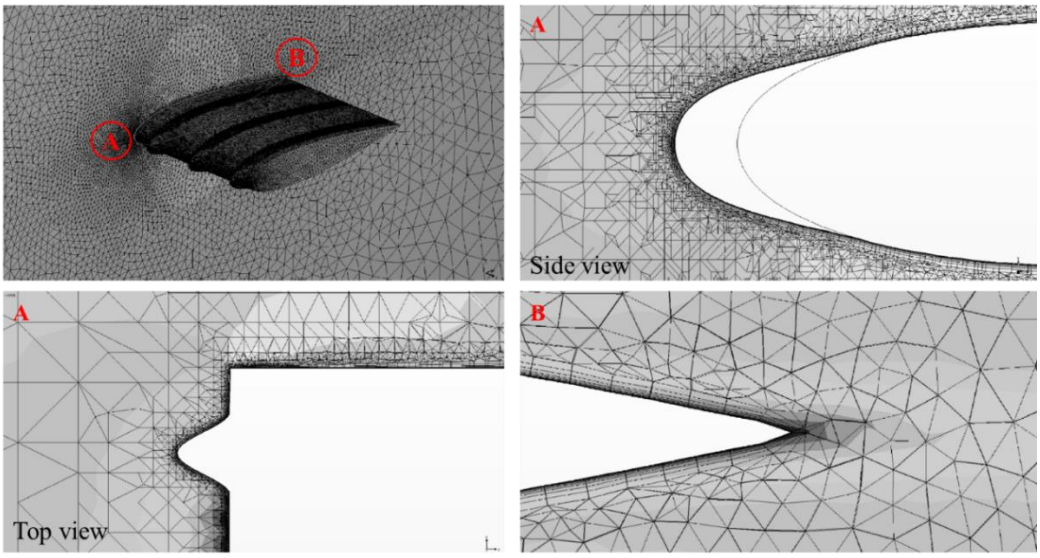

Figure 7. Meshing configuration for WLE wing with A, and B are leading edge and trailing edge that located at the symmetry plane.

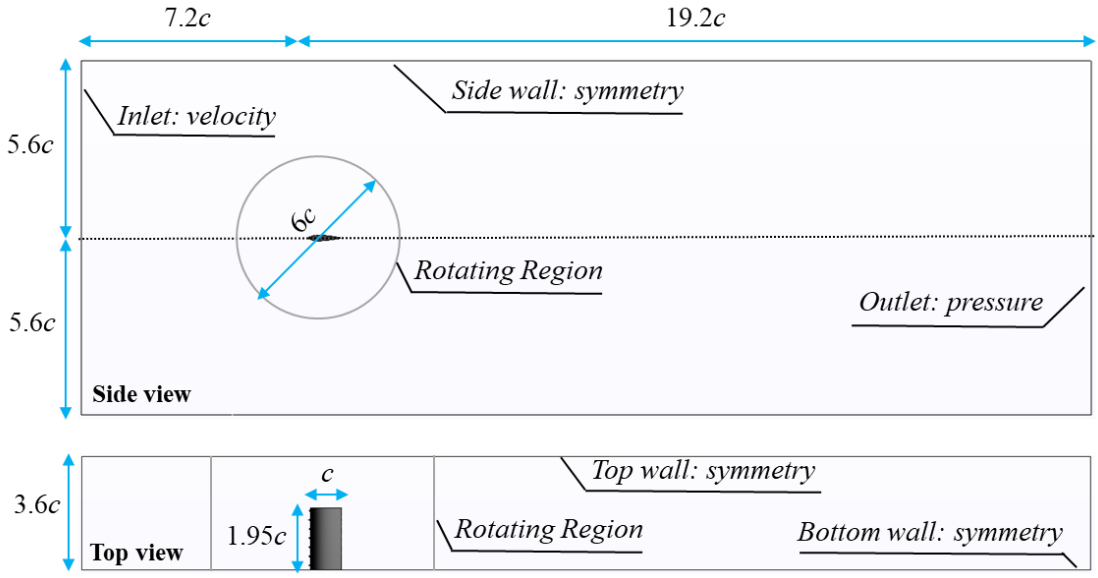

Figure 8. Domain simulations unsteady case and its boundary condition (AR 3.9)

RESULTS AND DISCUSSIONS

Unsteady analysis of rectangular wing

Unsteady analysis of rectangular wings has been investigated exclusively during stall conditions at angles ranging from 25° to 35°. The *Cl* and *Cd* values at AR 3.9 are shown in Figure 9 in both steady and unsteady conditions. In this section, the experimental result for the steady case was reported for comparative purposes. The baseline wing produced results similar to the experimental findings at angles ranging from 25° to 35° during the upstroke motion. However, the *Cl* values were lower during the downstroke motion. Similarly, the *Cl* value during the upstroke motion of the WLE wing was identical to that of the stationary case for angles between 30° and 35°. The baseline wing had a lower *Cd* value than the steady case, however, the WLE wing produced results that were close to the steady case. Because the unsteady result at an angle of 30° during the upstroke motion was similar to the steady one, the pressure coefficient and velocity distribution at this angle were compared, as shown in Figures 10-11.

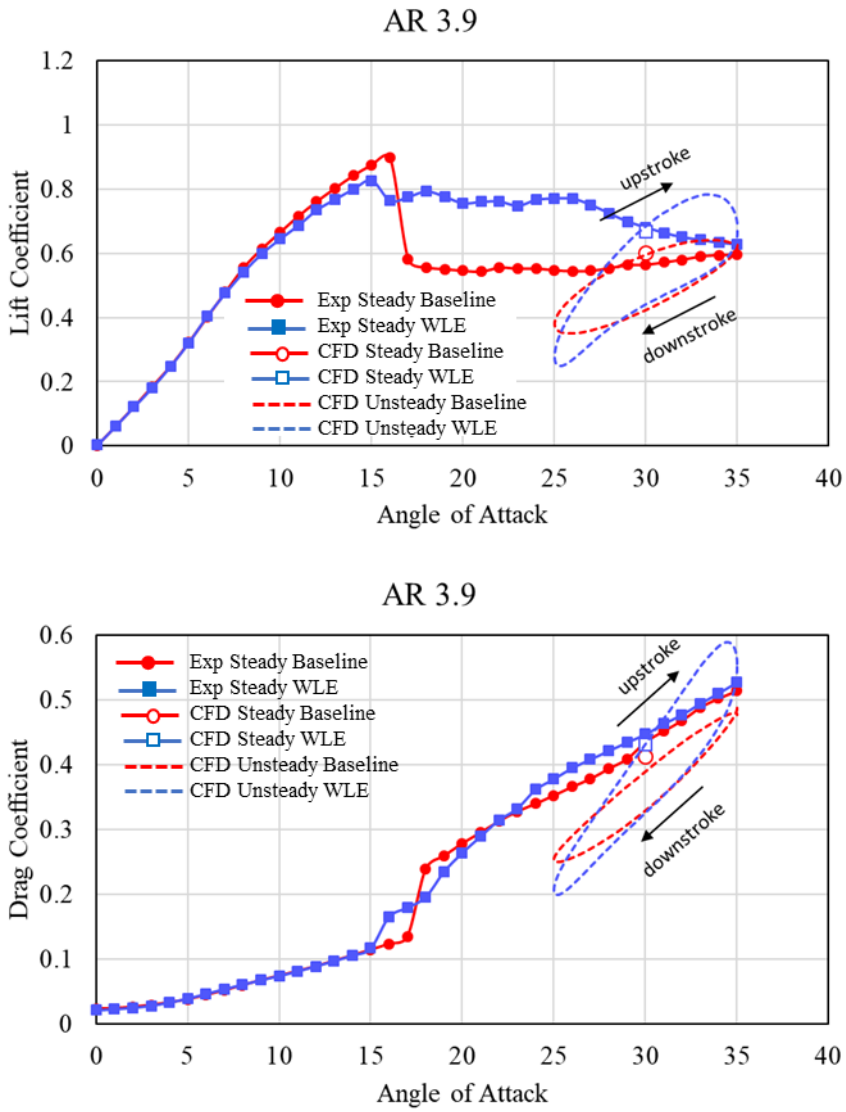

Figure 9. Lift coefficient (*Cl)* and drag coefficient (*Cd)* at AR 3.9

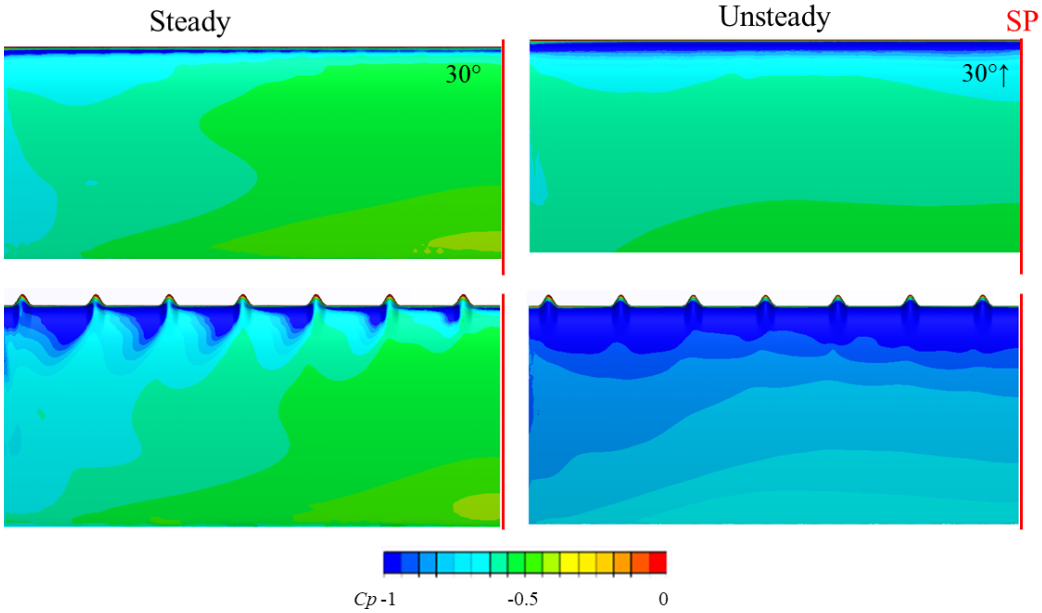

Figure 10. Pressure coefficient distribution of AR 3.9 at 30°

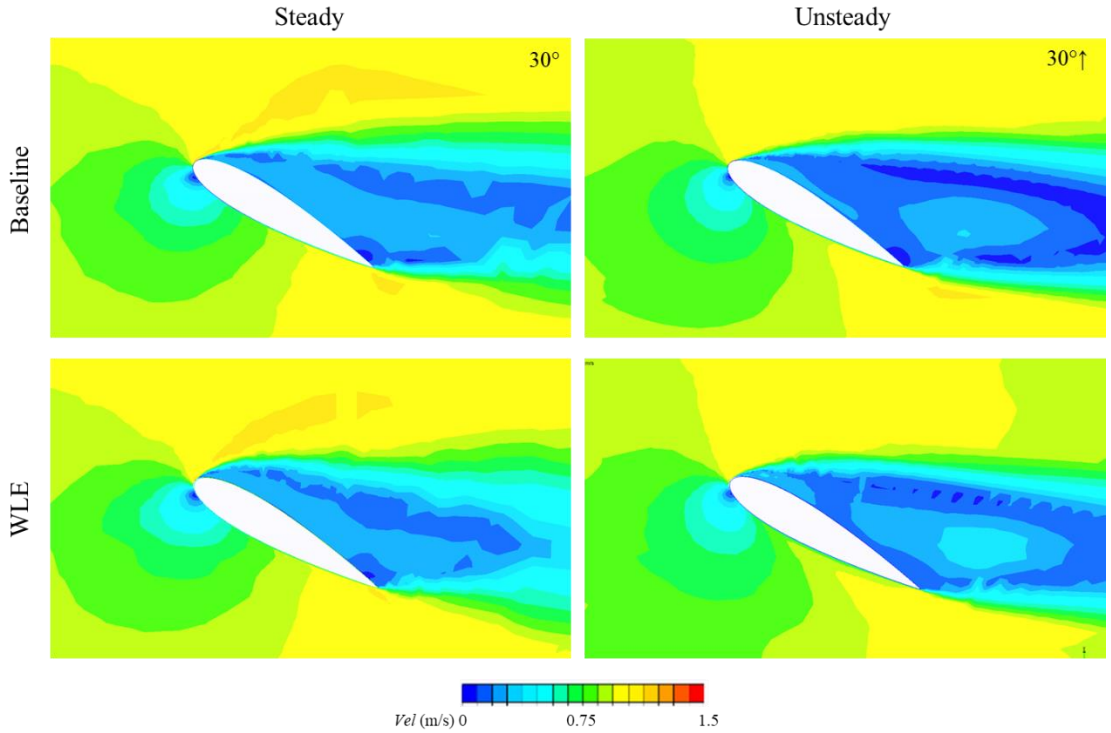

Figure 11. Velocity Magnitude distribution of AR 3.9 at angle 30°

Figure 10 shows the pressure coefficient at 30° at AR 3.9, demonstrating that the WLE wing has lower pressure than the baseline wing in both steady and unsteady conditions. Significant dissimilarities were identified in the WLE wing during upstroke motion, with low pressure dominating its surface, implying that the flow went through the wing surface more easily, perhaps delaying separation. The distribution of velocity magnitude in the mid span is illustrated in Figure 11, revealing that the separation point is towards the leading edge, with a somewhat delayed separation point on the WLE wing and a narrower wake region.

Figure 12 illustrates the *Cl* and *Cd* for AR 5.1 wing, the WLE wing, had higher *Cl* than the baseline wing during upstroke motion at angles ranging from 25° to 35° after stall conditions. For angles 30°-35°, the *Cl* values for the baseline wing were consistent during upstroke motion. The WLE and baseline wing displayed comparable tendencies during downstroke action. At a 30° angle of attack, the steady and unsteady examples produced the same *Cl* value, suggesting a comparison as illustrated in Figures 13-14.

Figure 13 shows the pressure coefficient (*Cp*) on the suction wing surface, the left side represents the steady case distribution of *Cp*, whereas the right side illustrates the unsteady case result during upstroke motion. The baseline wing revealed no significant dissimilarities between the steady and unsteady cases, whereas the WLE wing showed a significant difference in the pressure coefficient distribution between the steady and unsteady cases. The surface was almost entirely covered by a deep blue color that indicating a decreased pressure on the surface. As a result, the flow through the WLE wing surface was smoother during upstroke motion. An important observation was that the inconsistent motion performed better in this condition.

Because of the size limitation of circular water channel, the experimental investigation can only be performed for AR less than 5. Rohmawati et al [19] investigated the effectiveness of AR, finding that AR 7.9 has the best performance. This AR is comparable to that of humpback whale flippers in 3.6-7.7 [20]. The *Cl* and *Cd* of numerical results the rectangular wing at AR 7.9 at steady case at angles 20°-30° and unsteady case at angles 25°-35° are shown in the Figures 15-17 below.

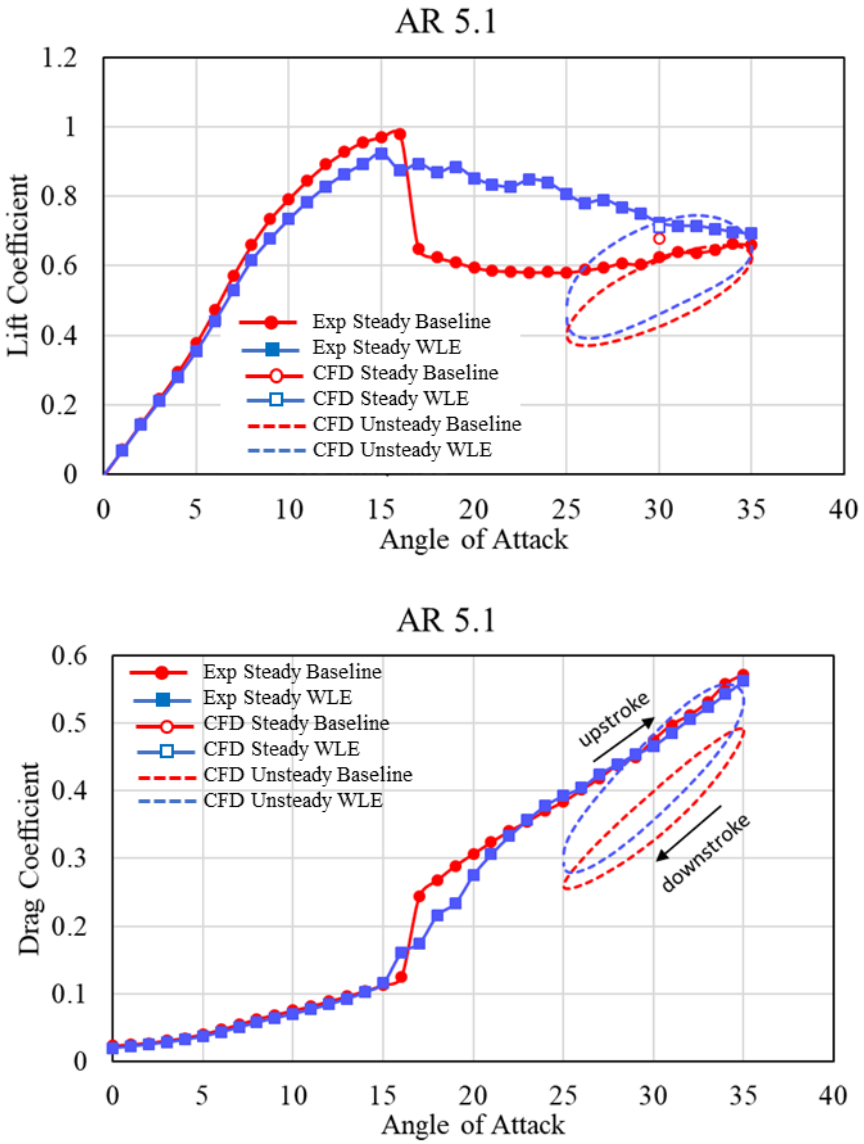

Figure 12. Lift coefficient (*Cl)* and drag coefficient (*Cd)* at AR 5.1

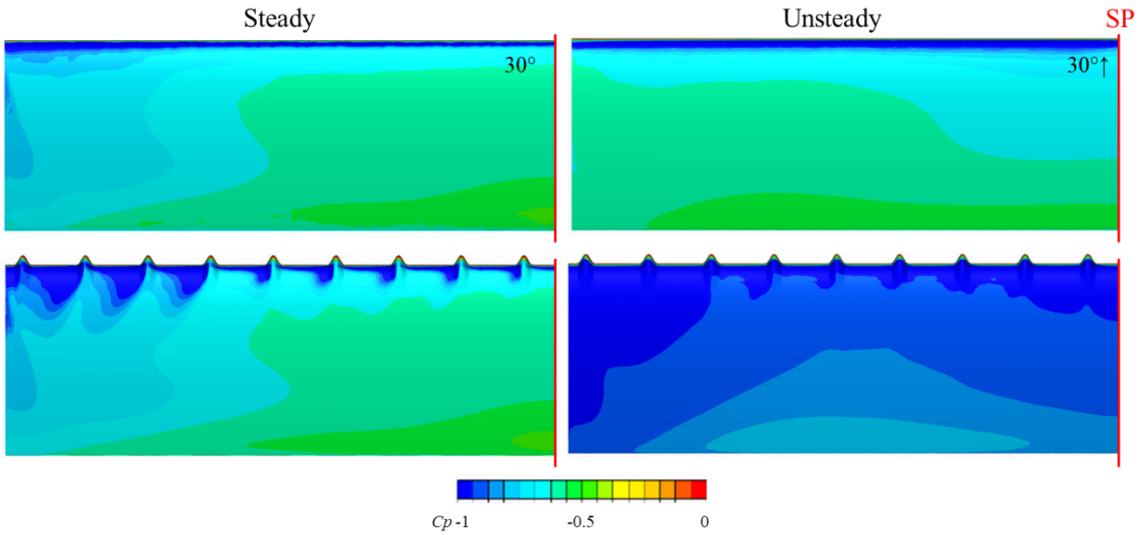

Figure 13. Pressure coefficient distribution of AR 5.1 at 30°

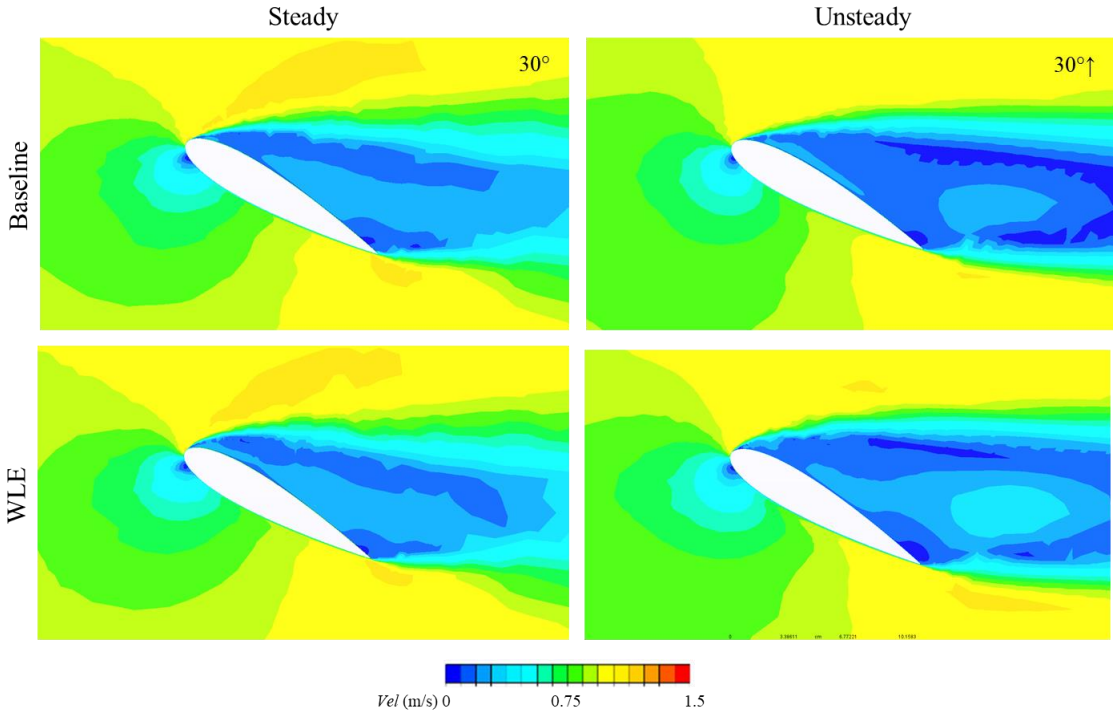

Figure 14. Velocity Magnitude distribution of AR 5.1 at 30°

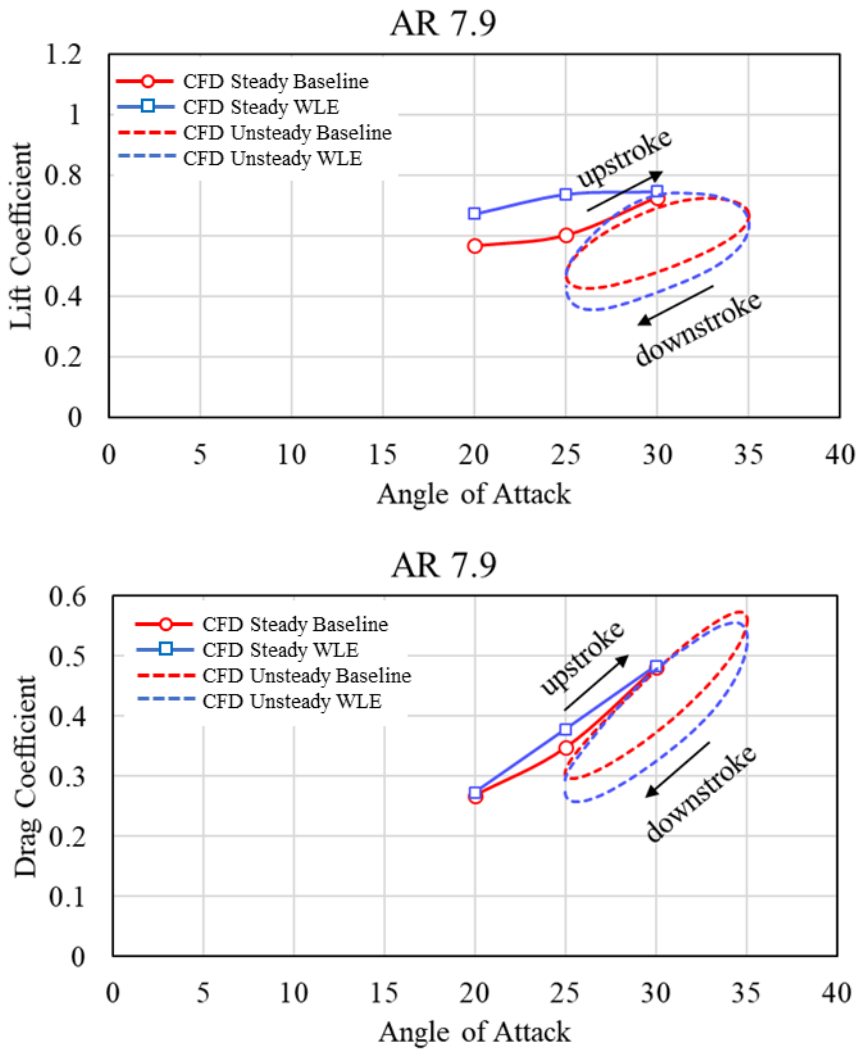

Figure 15. Lift coefficient (*Cl)* and drag coefficient (*Cd)* at AR 7.9

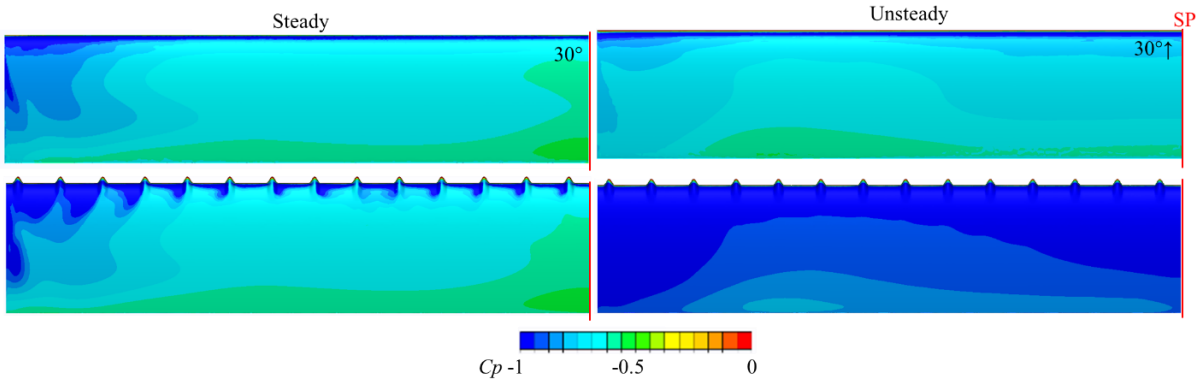

Figure 16. Pressure coefficient distribution of AR 7.9 at 30°

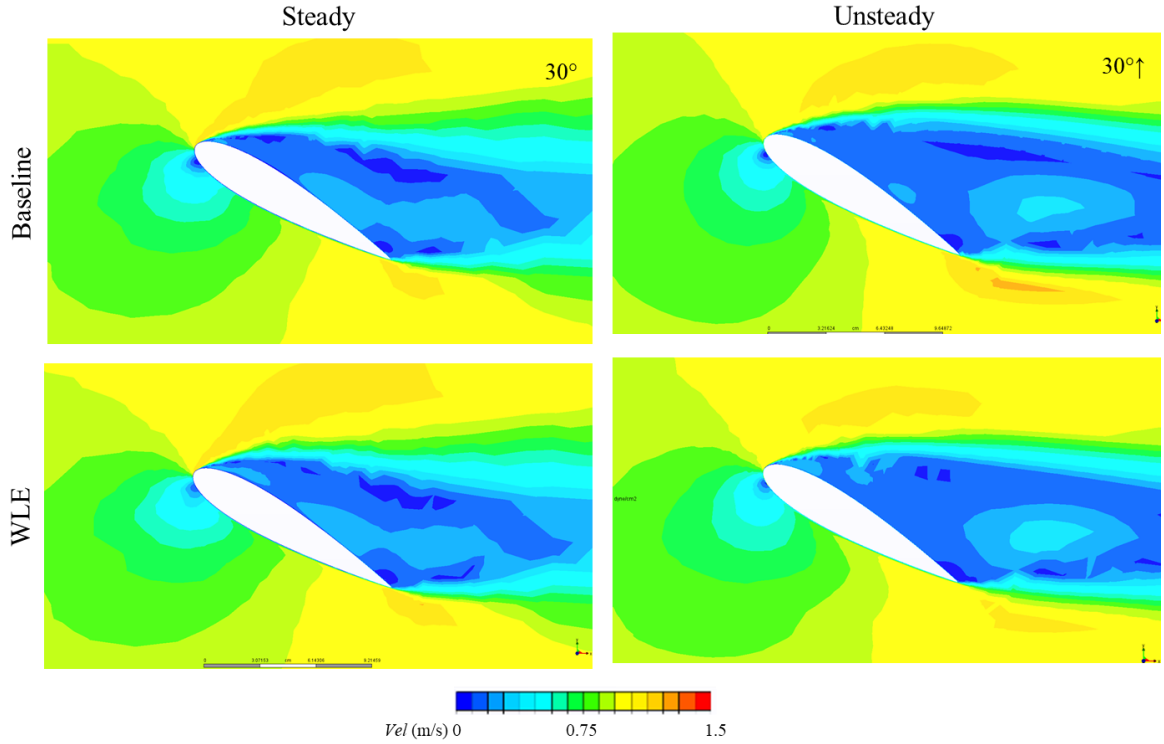

Figure 17. Velocity Magnitude distribution of AR 7.9 at 30°

A graph illustrating *Cl* and *Cd* for steady and unsteady circumstances at AR 7.9 can help explain how the WLE effect impacts aspect ratio in unsteady conditions. Previous research [19] found that AR 7.9 performed better than other aspect ratio modifications. However, in unsteady conditions, AR 7.9 performed more severe than the baseline wing.

The impact of the WLE on rectangular wings with aspect ratios of 3.9, 5.1, and 7.9 was observed in unsteady conditions. The consistent phenomena were found in aspect ratios (AR) 3.9 and 5.1, where the WLE wing has prior performance than the baseline wing in the post-stall condition. Meanwhile, there are no substantial dissimilarities between the baseline and WLE wings for AR 7.9 wing. A similar tendency was discovered in reference [21], where the WLE wing performed best during upstroke motion rather than downstroke action. The presence of WLE influences fluid flow properties where a twisted stream-wise vortical flow around the WLE was identified during both upstroke and downstroke motion, with the vortical flow being stronger during upstroke motion than downstroke motion.

The results of this study suggest that modifying the geometry of the utilized foil from a rectangular wing to a tapered one may be a promising approach for improving the

performance of systems that rely on aerodynamic lift, such as wind turbines or fin stabilizers. Tapered wings are known to have a more efficient lift-to-drag ratio compared to rectangular wings, which could potentially result in increased energy efficiency and stability of these systems. Furthermore, the investigation of different wing geometries can provide insights into the fundamental principles of fluid mechanics and help identify optimal designs for various applications. Therefore, further research on the impact of wing geometry on fluid flow characteristics is warranted, particularly in the context of practical applications.

CONCLUSIONS

The purpose of this study was to investigate the influence of the WLE on the unsteady performance of a rectangular wing with three different aspect ratios (AR) of 3.9, 5.1, and 7.9. It was revealed that the WLE wing exceeded the baseline wing in the post-stall scenario for aspect ratios of 3.9 and 5.1. In contrast, no significant variations were noticed for the AR 7.9 wing. These results are identical to those reported in prior references [19, 21], where the impact of WLE on a rectangular wing was explored and greater performance was seen during upstroke motion rather than downstroke motion. These findings imply that the effect of WLE on wing performance is strongly dependent on the AR and the wing motion.

ACKNOWLEDGEMENTS

The authors are grateful to Prof. Yasuaki DOI and Prof. Hidemi MUTSUDA for their support during the research at Hiroshima University in Japan.

DECLARATION OF CONFLICTING INTERESTS

The author(s) declared no potential conflicts of interest with respect to the research, authorship, and/or publication of this article.

FUNDING

The author(s) disclosed receipt of the following no financial support for the research, authorship, and/or publication of this article.

REFERENCES

[1] No. 2935 Whale Aerodynamics: “No. 2935 Whale Aerodynamics:,” n.d. https://www.uh.edu/engines/epi2935.htm.
[2] J. M. B. Frank E. Fish, “Hydrodynamics Design of The Humpback Whale Flipper.” Journal of Morphology 225 : 51 - 60 (1995), pp. 51–60, 1995.
[3] F. E. Fish, P. W. Weber, M. M. Murray, and L. E. Howle, “The Tubercles on Humpback Whales ’ Flippers : Application of Bio-Inspired Technology,” vol. 51, no. 1, pp. 203–213, 2011.
[4] F. E. Fish, “Biomimetics : Determining engineering opportunities from nature,” Proc. SPIE, vol. 7401, pp. 1–11, 2009.
[5] D. S. Miklosovic and M. M. Murray, “Experimental Evaluation of Sinusoidal Leading Edges,” J. Aircr., vol. 44, no. 4, pp. 2–5, 2007.
[6] D. S. Miklosovic, M. M. Murray, L. E. Howle, and F. E. Fish, “Leading Edge Tubercles Delay Stall on Humpback Whale (Megaptera Novaeangliae) Flippers,” Phys. Fluids, vol. 16, no. 5, pp. 39–42, 2004.

[7] H. T. C. Pedro and M. H. Kobayashi, "Numerical Study of stall delay on humpback whale flippers," no. January, pp. 7–10, 2008.
[8] H. Johari, C. Henoch, D. Custodio, and A. Levshin, "Effects of Leading Edge Protuberances on Airfoil Performance," AIAA J., vol. 45, no. 11, pp. 2634–2642, 2007.
[9] H. Arai, Y. Doi, T. Nakashima, and H. Mutsuda, "Hydrodynamic Performance of Wing with Wavy Leading Edge," Adv. Marit. Eng. Conf. 4th Pan Asian Assoc. Marit. Eng. Soc. Forum, no. 2009, pp. 978–981, 2010.
[10] H. Arai, Y. Doi, T. Nakashima, and H. Mutsuda, "A Study on Stall Delay by Various Wavy Leading Edges," J. Aero Aqua Bio-mechanisms, vol. 1, no. 1, pp. 18–23, 2010.
[11] Z. Wei, J. W. A. Toh, I. H. Ibrahim, and Y. Zhang, "Aerodynamic characteristics and surface flow structures of moderate aspect-ratio leading-edge tubercled wings," Eur. J. Mech. / B Fluids, vol. 75, pp. 143–152, 2019.
[12] Y. Wang, W. Hu, and S. Zhang, "Performance of the bio-inspired leading edge protuberances on a static wing and a pitching wing," J. Hydrodyn., vol. 26, no. 6, pp. 912–920, 2014.
[13] S. Wang, D. B. Ingham, L. Ma, M. Pourkashanian, and Z. Tao, "Computers & Fluids Numerical investigations on dynamic stall of low Reynolds number flow around oscillating airfoils q," Comput. Fluids, vol. 39, pp. 1529–1541, 2010.
[14] A. Buchner, M. W. Lohry, L. Martinelli, J. Soria, and A. J. Smits, "Dynamic stall in vertical axis wind turbines : Comparing experiments and computations," J. Wind Eng. Ind. Aerodyn., vol. 146, pp. 163–171, 2015.
[15] A. Orlandi, M. Collu, S. Zanforlin, and A. Shires, "3D URANS analysis of a vertical axis wind turbine in skewed fl ows," J. Wind Eng. Ind. Aerodyn., vol. 147, pp. 77–84, 2015.
[16] H. R. Karbasian and K. C. Kim, "Numerical investigations on flow structure and behavior of vortices in the dynamic stall of an oscillating pitching hydrofoil," vol. 127, no. February, pp. 200–211, 2016.
[17] S. Wang, L. Ma, D. B. Ingham, M. Pourkashanian, and Z. Tao, "Turbulence Modelling of Deep Dynamic Stall at Low Reynolds Number," vol. II, 2010.
[18] K. Gharali and D. A. Johnson, "Dynamic stall simulation of a pitching airfoil under unsteady freestream velocity," J. Fluids Struct., vol. 42, pp. 228–244, 2013.
[19] Rohmawati, I., Arai, H., Mutsuda, H., Nakashima, T., and Mahmud, R., "Optimizing Effect of Wavy Leading Edge (WLE) in Rectangular Wing and Taper Wing.", J. Mech. Eng. Science and Innovation, vol.1 no 2, 2021.
[20] B. F. N. (editors) D. T. H. New, Flow Control Through Bio-Inspired Leading Edge Tubercles. 2020.
[21] Rohmawati, I., Arai, H., Nakashima, T., Mutsuda, H., and Doi, Y., "Effect of Wavy Leading Edge on Pitching Rectangular Wing.", J. Aero Aqua Bio-mechanism vol. 9, issue 1, 2020.